Journal of Electronic Materials, Vol. 4, No. 5, 1975

VOID INITIATION, GROWTH, AND COALESCENCE IN DUCTILE FRACTURE OF METALS

H. G. F. Wilsdorf

Department of Materials Science
University of Virginia
Charlottesville, Virginia 22901

(Received March 25, 1975)

Ductile fracture in metals and alloys occurs through the coalescence of voids in the necked region of the specimen. While considerable information exists on the propagation of cracks, the mechanism of their initiation is still unclear. This paper reports on in situ electron microscope investigations aimed at an elucidation of crack initiation and the enlargement of crack nuclei to final rupture. Single crystal ribbons of silver 0.5 - 7.0 μm thick were pulled to fracture inside of a high voltage electron microscope (HVEM). After considerable necking, cracks initiated at the edges; their propagation occurred by the formation of microcracks ahead of the macrocrack, followed by the growth of the microcracks and finally their coalescence. These in situ experiments were complemented by stress-strain data obtained from fractured austenitic 304 stainless steel foils; subsequent examination of fracture surfaces in a scanning electron microscope allowed the accurate measurement of intervoid spacings. Inter-particle spacings were determined by HVEM. It was found that the average void density is 100 times larger than the average particle density. The combination and analysis of all experimental data led to a detailed model of void initiation and growth, which is based on a dislocation-vacancy mechanism and crystal plasticity.

Key words: metals, ductile fracture, voids.

Introduction

Metals are known to fail in a brittle or ductile mode. Intensive efforts to understand brittle fracture go back to the year 1924 when Griffith published his fundamental thoughts relating fracture stress to surface energy. In contrast, ductile fracture studies have received only scant attention until the late fifties. The reasons for this neglect are manyfold: While mathematical treatments of brittle fracture are based on well defined concepts in elasticity theory, ductile failure had to be treated on the basis of plasticity theory, which could not provide the exacting formulation needed to obtain a deeper insight. Further, brittle failure can be treated adequately by calculating the energy to propagate a crack; in contrast, in ductile failure the onset of fracture is of utmost importance. Through progress in experimental techniques, metallurgical investigations have greatly contributed to the understanding of crack initiation. The present investigation aims at developing a new aspect of crack nucleation in pure metals and alloys as well as providing microstructural details on crack propagation.

The fact that ductile fracture takes place after an appreciable amount of plastic flow points to the need for detailed information on the specimen's deformation history. Since glide is an anisotropic phenomenon the crystal structure of the specimen has to be considered. After a clarification of the glide geometry, the lattice defects responsible for plastic flow must then be studied. Dislocation theory in combination with direct observation techniques for dislocations are powerful tools in exploring fracture initiation and growth in the submicroscopical regime. Clearly, the objective of this Conference, namely to focus on the relationship between crystal defects and physical behavior is pursued in our approach to further the understanding of ductile fracture in pure metals and alloys.

Discussion of General Concepts

It is now generally accepted that ductile fracture begins with the formation of voids and that it proceeds by

the growth of these voids until the failure is completed through their coalescence. A metallic specimen which is being deformed in tensile loading will experience sooner or later plastic instabilities. In the case of a cylindrical tensile specimen, necking will occur, i.e. the cross-section of the specimen will be reduced sharply near the middle section. The stresses acting on the necked-down portion of the specimen have changed from unidirectional to triaxial. Also, necking causes greater work hardening in this part of the specimen and it is here where the first void formation has been observed. The growth of voids takes place preferentially in the center portion of the neck and the first cracks have been observed to develop in directions perpendicular to the stress axis of the specimen. The cracks spread from the center to the outside; however, a short distance before reaching the surface, shear in the directions of highest stress will take place producing a shear lip. This completes the typical ductile fracture of a cylindrical tensile specimen, usually called "cup and cone" fracture. In comparison to the rest of the specimen the necked region represents a severe plastic instability and furthermore has experienced extensive work hardening.

Although ductile fracture is hardly of practical consequence in service failures of structural components, rupture is by no means a purely academic matter. Failure in the ductile mode may occur in deformation processing such as in wire drawing, rolling, extrusion or others. It appears that due to the industrial interest in ductile fracture, materials of commercial purity have been investigated rather than high purity metals and alloys as has been customary in physical metallurgy. As will be shown, the choice between these two purity grades has had a significant influence on the current understanding of crack initiation in ductile metals.

Gorland and Plateau (1) have pointed out that the strain energy relief due to void formation must be sufficient to produce the surface energy needed to create the new surfaces. If one assumes as void nucleation sites the presence of second phase particles in a metal matrix one can write (1) for the stress required to initiate a void

$$\sigma = \frac{1}{\alpha} \left(\frac{E\gamma}{D}\right)^{1/2} \quad (1)$$

with σ the nominal stress in the matrix, E the modulus of elasticity, D the particle diameter and a factor α accommodating the stress concentrations around the particle. Clearly, the value for γ is dependent on both the surface energies of matrix and particle as well as on the interfacial energy (2). Relatively few experimental investigations are known to have been conducted to establish in a quantitative and comprehensive manner this relationship. The best study of this type has been published by Broek (3) who made extensive measurements on fourteen aluminum alloys. His work confirmed the contention that second phase particles act as nucleation sites for voids, and there are now numerous publications by other authors providing details of the mechanisms responsible. All this work represents a very valuable contribution to the understanding of ductile fracture.

The processes that lead to the initiation of ductile fracture in pure metals and alloys are less clear. These materials are known to undergo very high reductions in area and often fracture with a chisel point. However, also in specimens of high purity metals and alloys the presence of dimpels has been observed on their fracture surfaces which is evidence for the validity of the sequence of void initiation, void growth and void coalescence. With the advent of dislocation theory a number of dislocation models explaining void formation have been proposed. Either, dislocation interactions with obstacles or dislocation reactions form the basis of these models. While it makes sense to apply them to metals containing second phase particles, since here dislocation interactions with particles will take place in the early stages of deformation, their application to void initiation in pure metals is not possible. It must be recalled that rupture is preceded by severe necking which means that void initiation is taking place in a highly work hardened area of the specimen. Arguments why necking is not being caused by void formation have been given by Broek (3). It is then clear that void initiation is found in that part of the specimen which has been undergoing the largest work hardening.

It is an established fact that with increasing work hardening the dislocation density also increases. The basic relationships that are pertinent to strain hardening are

$$\gamma = \rho b l \ldots \quad (2)$$

and

$$\tau = \sqrt{\rho} G b C \ldots \quad (3)$$

These equations show that the shear strain γ is proportional to the dislocation density ρ and the shear stress τ is proportional to the square root of the dislocation density. b is the Burgers vector, l the average distance traveled by a dislocation, G the modulus of rigidity and C a parameter which is dependent on the specific work hardening model used. Dislocation densities in the necked portion of a tensile specimen are estimated to be 10^{10} dislocations/cm^2 or higher. In crystals which have been deformed with normal strain rates the majority of the dislocations is arranged in sub-boundaries and glide dislocations can move at normal overall dislocation densities through distances in the micron range. However, this distance is becoming smaller with increasing work hardening and it appears most doubtful whether any of the dislocation models proposed for void initiation is applicable under these conditions. A popular model is predicated on the presence of pile-ups against obstacles. Provided the obstacle will stand the stress produced by, say 25 dislocations, it is conceivable that the first few dislocations at the head of the pile-up will coalesce and form a void nucleus. Despite the large volume of work in the field of work hardening, pile-ups at high dislocation densities have not been observed experimentally. As has been shown earlier (4) even at dislocation densities of 2×10^8 dislocations/cm^2 pile-ups interfere with each other so that the effect of the superimposed stress fields of single dislocations comes not to bear on the the stress concentration at the head of the pile-up in a significant manner.

For a realistic appraisal of the dislocation patterns in a highly workhardened area one has to take into account the strain rate. The decreasing cross-section of the specimen in the neck is responsible for an increased strain rate $\dot{\varepsilon}$. It follows from equation (2) that

$$\dot{\varepsilon} = \rho b v \qquad (4)$$

with v the average dislocation velocity. Since the actual strain rate in the necked portion of the specimen can easily be ten times larger than the nominal strain rate imposed on the overall specimen by the tensile machine, the dislocation mobility must be affected. It must be concluded from equations (2), (3), and (4) that the dislocations are getting less mobile with continued formation of the neck. One can anticipate that instead of well defined sub-boundaries irregular dislocation clusters will develop which then represent internal stresses of finite size.

Brief Review of Experimental Techniques

Microstructural investigations for the study of fracture mechanisms have been relying heavily on observations of fracture surfaces with the scanning electron microscope (SEM). Although the resolution of this technique is only 1.5×10^{-6} cm and mostly not better than 2.5×10^{-6} cm, it has the great advantage that both fracture surfaces can be directly viewed over a wide range of magnifications, namely between 500 X and 40,000 X. This means that measurements can be made from large areas without the preparation of replicas from the rather rough surface as would be required for transmission electron microscopy (TEM). Excellent articles reviewing the study of fracture surfaces have been published by Beachem (5) and Broek (6). The SEM becomes even more valuable when using it in conjunction with an energy dispersive X-ray analyser, thereby adding an analytical capability for determining the presence of elements from fluorine to higher atomic number elements in the surface.

Since the fracture mechanism is strongly dependent on the specimen's deformation history, the investigation of dislocations can be of great help. A summary of experimental techniques for dislocation studies pertaining to fracture has appeared elsewhere (7). May it suffice here to say that TEM for the investigation of ductile fracture appears to be of limited value since dislocation patterns at $\rho > 5 \times 10^{9}$ dislocation/cm^2 remain unresolved at reasonable specimen thickness; it is now clear that the real interest lies in dislocation patterns of $\rho > 10^{10}$ dislocation/cm^2.

However, a new approach was tried by using in situ straining of metal ribbons to fracture inside a high voltage electron microscope (HVEM). Due to the increased transmission power of high energy electrons, specimen thickness can be increased to about 0.5 - 3.0 μm depending on the atomic number of the specimen under investigation. With increased thickness of a miniature tensile specimen one might expect a dislocation behavior approaching that of bulk specimens in plane stress. The technique used in this investigation employed single crystal ribbons of uniform thickness and width and permitted them to be deformed at controlled elongation rates to fracture. The propagation of cracks was to be recorded at magnifications of up to 80,000 X with a frame speed of 30/sec on video tape. A detailed description of the HVEM in situ straining technique including the preparation of suitable specimens has been published previously by R. Bauer, R. Lyles, Jr. and H. G. F. Wilsdorf (8).

Experimental Results

The first part of the void initiation - growth - coalescence sequence in alloys containing second phase particles, namely the nucleation of voids, has now been well investigated and it is understood in considerable detail. However, this mechanism cannot operate in pure metals and alloys. It had been suggested earlier that voids may possibly be formed where heavy plastic deformation has occurred (9) but conclusive evidence at the microstructural level for such a mechanism is lacking. This is hardly surprising since void initiation is a phenomenon taking place at the submicroscopical level, and any technique capable of discerning useful details would have to have the capability of resolving crystal defects or multiples thereof. It was found that in situ fracture experiments inside a HVEM permitted this to be done. Before reporting the results obtained with our direct viewing technique, some statistical information will be given.

The measurements on which the statistical data are based have been made on fractographs taken with the SEM. Electron fractography has contributed greatly to the development of our present understanding of fracture initiation in ductile metals and alloys containing second phase

particles. In order to correlate these experiments with the straining of thin foils in the HVEM, foils of 304 stainless steel ranging in thickness from 4 μm to 1020 μm were fractured at a crosshead speed of 8.33×10^{-4} mm/sec in an INSTRON tensile testing machine. The foils were prepared from specially selected stock and annealed for recrystallization in the austenitic range yielding grain sizes between 15 and 30 μm. Details of the preparation technique and the testing as well as the mechanical properties determined were published earlier (10).

The fracture surfaces of tensile specimens 99, 138, and 168 μm thick, all of which showed transverse necking, were investigated by SEM. The inter-void spacing were found to be between 2.0 μm and 4.3 μm. These values had then to be compared with inter-particle spacings. Electron transparent foils of the material were prepared by electro-polishing and carefully screened in the HVEM. Second phase particles of diameters between 0.3 μm and 10 μm were easily seen and inter-particle distances from 7.4 μm to 16.1 μm were obtained. In addition, thinner specimens, say, 500 Å to 1,000 Å thick were checked for small precipitates by TEM and occasionally particles of 100 Å to 200 Å were discernable. Distances between these very small particles were mostly found to be in the order of 100 μm with a few scattered groups containing about 5 particles with interparticle distances in the order of 1 μm. Since the voids occupy rather uniformly the whole fracture surface this type of distribution pattern cannot be associated with the void arrangement observed on fracture surfaces of stainless steel; a typical distribution is shown in the fractographs of Figs. 1a and 1b.

A careful examination of the "dimples" in the fractographs (representing one geometrical half of all voids in the fracture surface) showed the presence of small numbers of second phase particles which were always associated with voids. Also, other geometrical features were seen at the bottom of the dimples. In order to clarify the suspicion that they were possible caused by impurity aggregates, energy dispersive X-ray analysis was employed. Traces taken from the bottom of the dimples were compared with those obtained from the matrix but no difference was found. Second phase particles, recognizable in fractographs by their darker

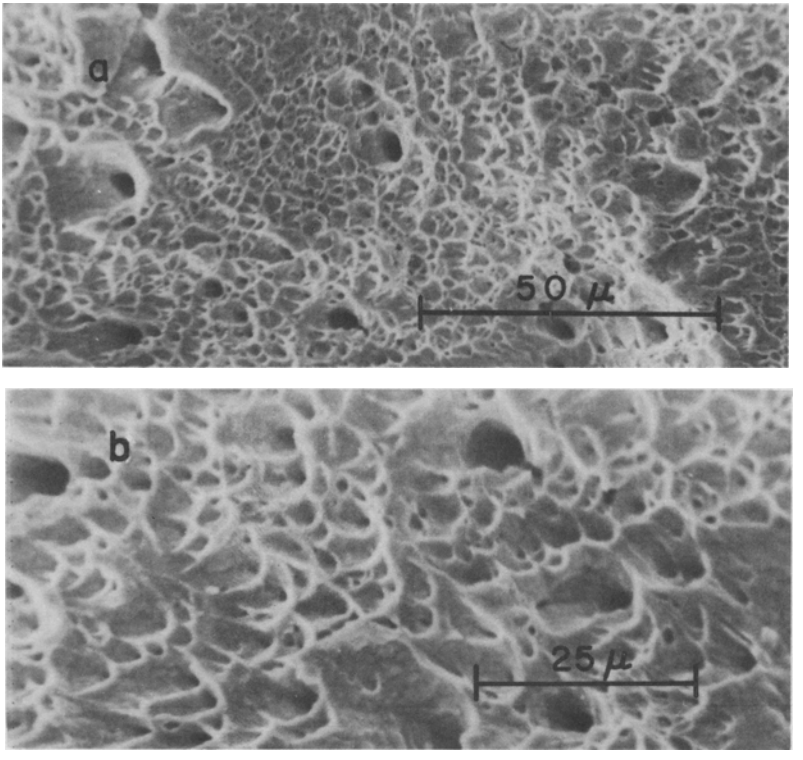

Fig. 1a and 1b. Void arrangement in fracture surface of 1 mm thick stainless steel foil.

color, give rise to significantly different traces as reported elsewhere (11).

The SEM study of fracture surfaces has shown that a 1:1 ratio of second phase particles to voids does not exist in austenitic 304 stainless steel foil prepared from special grade stock. Instead, the void density was found to be greater by a factor of 100 than the particle density. Clearly, an additional, different mechanism other than void initiation at second phase particles is indicated.

A HVEM investigation was designed to strain well characterized single crystals to fracture inside the microscope and to film the void initiation - growth - coalescence

sequence at magnifications which would permit the observation of lattice defects. The HVEM at the University of Virginia allows for radial entry into the specimen chamber which greatly facilitated the construction of a tensile stage with precision elongation control. Suitable specimens were obtained by the growth of silver single crystal ribbons through ion reduction (12). Crystals $1 - 5 \times 10^{-1}$ cm long, $0.1 - 1 \times 10^{-1}$ cm wide and $0.2 - 7 \times 10^{-4}$ cm thick were mounted on a soft copper support which was then attached to the grips of the tensile stage. With deformation of the copper foil the silver crystal was also elongated and continuously observed through an opening in the support. The elongation rate of the machine was variable between 1×10^{-6} cm/sec and 1×10^{-1} cm/sec.

The crystal ribbons had a <110> direction parallel to the tensile axis and their large surface was parallel to an octahedral plane. Depending on the elongation rate, the reduction of area at fracture was determined by SEM to range from 15% to 90%. The crystals necked down and a substantial amount of plastic deformation occurred in the neck before rupture. An analysis of the glide geometry has been made by Lyles (12). He found that a predictable rotation around an axis perpendicular to the large surface had always taken place leading to a final stress axis of the crystals in the neck parallel to <211>.

As shown schematically in Fig. 2, fracture started in the necked portion of the crystal beginning from one edge and propagating under an angle of approximately 60° against the stress axis until the failure was completed. The most significant observation however, was the formation of microcracks in front of the propagating macrocrack. The microcracks were initiated in the most heavily workhardened portion of the crystal which was due to transverse necking visible to about 10^{-3} cm in front of the macrocrack.

The initiation of microcracks took place at distances from each other that were amazingly similar. Consequently, it was predictable where the next microcrack would be formed which aided greatly in the screening of the specific area where the event was going to take place. The regular spacing of nucleation sites for the microcracks makes it *per se* highly improbable that they are caused by second

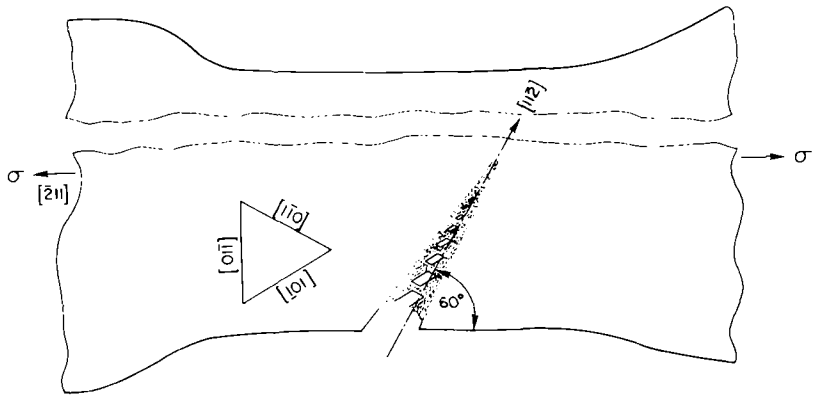

Fig. 2. Schematic representation of glide geometry in relation to propagating crack.

phase particles; searching for these, no inclusions were found in the thinned forward region before fracture nor after the coalescence of the microcracks was completed.

In situ straining in conjunction with a low light level video tape recording system permitted direct recording of the dynamic processes leading to the development of a sizeable microcrack. The sequence of events can be followed with the help of Fig. 3. Due to the difficulty of preparing a representative series of photographs from the TV screen, a schematic representation following photographs published earlier (13), was chosen. Figure 3a is provided to give an overview of an area ahead of the crack at time 0. Following, one can see in Fig. 3b at 4/30 sec that a narrow contrast area has been formed which at 7/30 sec has developed parallel to a <110> direction (Fig. 3c). Further elongations of the contrast zone can be seen at 10/30 sec and 14/30 sec in Figs. 3d and 3e. Finally, at 17/30 a slit parallel to the contrast zone has suddenly appeared. The sequence just described is typical for microcrack initiation at elongation rates of 10^{-5} and 10^{-6} m/sec and many similar sequences have been recorded on video tape.

The initiation of the microcracks in the transverse neck obviously is taking place under the action of a very

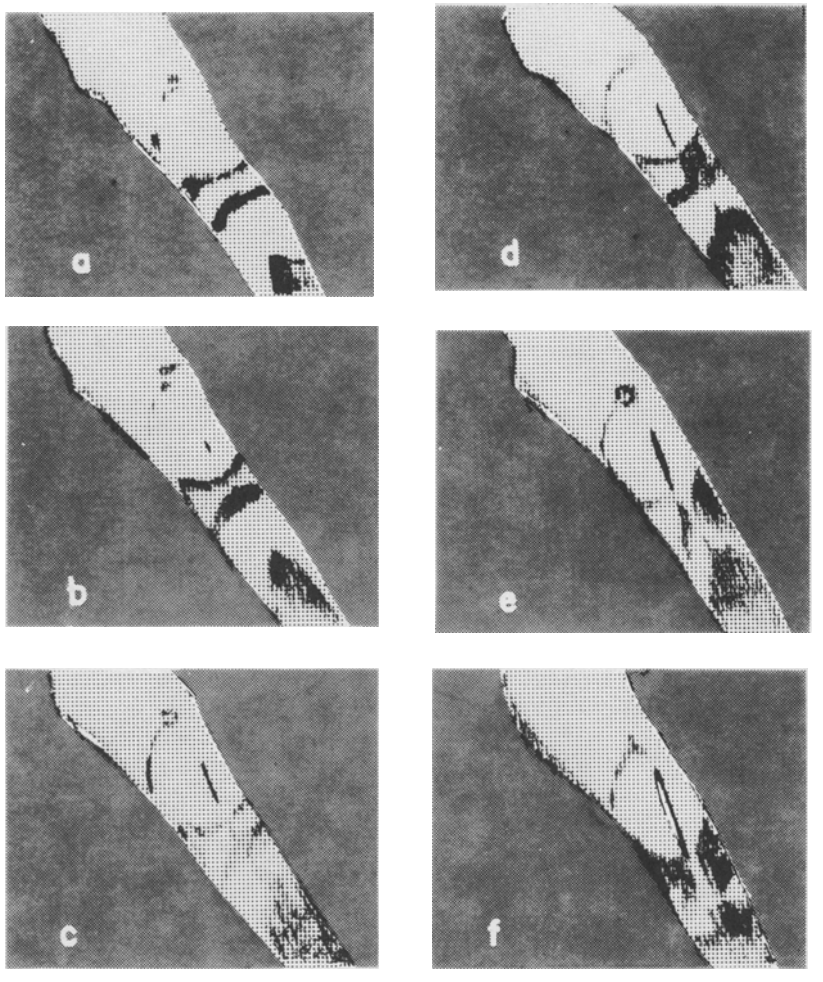

Fig. 3. Schematic time sequence illustrating micro-crack formation by micro-cleavage in front of propagating macrocrack. Drawings are made from individual frames of a video tape recording (13).

complex stress field. Nevertheless, it was found that the holes are being enlarged strictly by glide on only a few slip systems in accordance with established principles of plastic flow theories as has been shown by a detailed

analysis (12,13). The geometrical appearance of the holes is being enhanced with increasing size until they have the shape of parallelograms with their edges parallel to the two <110> directions that belong to the glide systems with the largest Schmid factor. The dislocation density continues to remain extremely high and it can be concluded that dislocations on active glide systems are leaving the crystal at the edges of the microcrack. Both, tensile and compressive stresses are acting, as evidenced by the step geometry of the edges, since the neighboring microcracks must have a significant influence on the stress distribution. The dislocation mobility is highest at the edges of the holes but with increasing hole size the area next to the edges is becoming thinner until the whole width of the transverse neck is electron transparent. At that stage the volume between the microcracks may properly be described as ligaments.

We are now coming to the final stage where the fracture is going to be completed and which is intimately related to the crack propagation mechanism. As has been mentioned earlier, this final stage is characterized by the coalescence of voids and attempts have been made in fracture mechanics to clarify this very complex phenomenon (14,15). In a bulk specimen the load near the crack tip is being carried by a void sheet (16). A close inspection of the topographical structure of fracture surfaces reveals that the material between voids has been reduced at this stage to very thin ligaments. Occasionally one finds an indication of geometrical shapes in the ligaments that one would have expected from slip on a few active glide systems. In general, however, the ligaments have irregular shapes which are related to the fracture mode (17).

Details of the plastic deformation of ligaments have been observed directly in silver ribbons by HVEM. As described above, the microcracks are initiated as very narrow slits parallel to <110>. They continue to grow in width and approach the shape of parallelograms with increasing size as the separating ligaments are becoming narrower. In the course of their reduction in width, they also are getting thinner, but not below a thickness of approximately 0.05 μm. The dislocation activity is very pronounced until the microcracks coalesce. A schematic

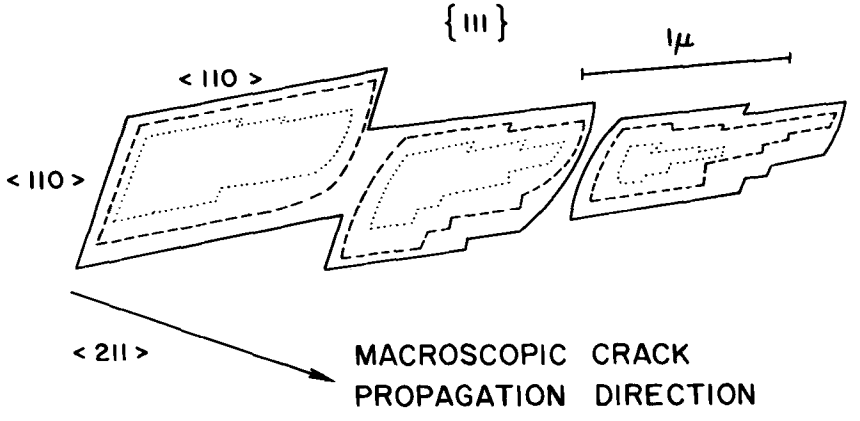

Fig. 4. Three stages in the growth of microcracks in thin silver crystals according to HVEM observations.

drawing, Fig. 4, illuminates three stages in the growth of microcracks.

Discussion and Conclusions

Results will be discussed that have been obtained by applying five experimental techniques to the void initiation - growth - coalescence sequence leading to ductile fracture. While the measurement of stress/strain values in a tensile machine, the observation of fracture surfaces by SEM and energy dispersive X-ray analysis, and the determination of inter-particle distances by TEM are conventional techniques, the HVEM in situ straining of well characterized tensile specimens to fracture combined with a light sensitive video-tape recording system was conducted for the first time.

The results from all techniques employed failed to indicate that the presence of second phase particles was a necessary prerequisite for void nucleation. Obviously, an alternative mechanism must be operative.

The formation of microcracks ahead of the macrocrack permitted a close examination of crack nucleation sites under dynamic conditions in the HVEM. The observation that narrow slits open up parallel to <110> in less than

0.1 seconds is interpreted as micro-cleavage. Tetelman (18) has concluded that micro-cleavage can be produced by macroscopic plastic deformation in iron -3% silicon and related the initiation as well as the blunting of cracks to the amount of plastic strain and temperature. In our case it is clear from HVEM observations that the crystal volume ahead of the crack is heavily work hardened, i.e., contains a dislocation density of 10^{11} to 10^{12} dislocations/cm . Contrast patterns showed that the dislocations are not continuously distributed but that they are concentrated in rather small volume elements with narrow areas of lesser density between them. The latter seem to correspond to the isotropic domains which were determined in heavily deformed metals by X-ray diffraction methods to be in the order of a few hundred angstroms (19). As already pointed out by Rogers (16), one may consider a highly work-hardened metal "as an elastically stressed solid on the verge of yielding since at any time it takes an infinitesimal increase in stress to cause plastic deformation and an infinitesimal decrease in stress to restore the solid to elastic behavior." It is known that the initiation of cleavage fracture occurs at the elastic plastic interface since it is here where the stress has its maximum value. The question that has to be considered is the availability of mobile dislocations. Gasca-Nevi and Nix have proposed a model for the mobile dislocation density that takes into account internal stresses which oppose dislocation motion (20). They showed that the fraction of mobile dislocations ρ_m/ρ falls off sharply with increasing normalized dislocation density $\rho(\frac{Gb}{t})^2$ as could be expected. Assuming a linear stress dependent velocity of the dislocations they found also that the strain rate goes through a maximum with increasing normalized dislocation density but declines sharply after it. All of these arguments are in support of the interpretation that micro-cleavage is responsible for the initiation of microcracks in pure metals and alloys.

In highly work-hardened metals the presence of vacancies or vacancy clusters can be expected (21,22). It is not unlikely that these might play an important part in triggering the micro-cleavage process. Our experimental data allow us to evaluate this possibility. Assuming that similitude exists between dislocation and vacancy distribution to follow the distribution of dislocations which

changes its scale as $1/(\tau - \tau_o)$ with τ and τ_o the applied and the frictional shear stress respectively. Data published by Bauer and Wilsdorf has shown that the inter-void spacing is decreasing with increasing stress (11) which strengthens the contention that a dislocation-vacancy - micro-void mechanism is most probably involved in triggering the micro-cleavage process. Due to the predominating diffraction contrast in front of the cracks, micro-voids would not be discernable even if present. However, prismatic dislocation loops were seen in fractured silver ribbons 5×10^{-5} cm thick near the crack flanks (23) which adds credibility to this proposal.

The growth of newly initiated slit-like microcracks takes place under very complex stress conditions since stress concentrations from neighboring microcracks will be imposed onto the applied stresses. However, the HVEM study shows that the development of holes with parallelogram-like shape in the ribbon can be explained perfectly on the basis of classical principles of crystal plasticity. On the other hand, voids growing in the void sheet of bulk crystals have predominantly rounded features. Are the results obtained from the deformation of thin crystals in the HVEM applicable to void growth in bulk fracture? Clearly, the constraints in the third space direction are missing in the in situ experiments and also the three-dimensional space distribution of voids during the growth process is not present. In order to be able to judge how far our results obtained from thin crystals are applicable to the mechanism of ductile fracture in general, thin silver ribbons 2×10^{-4} cm thick were strained to fracture in a precision bench straining device at the same elongation rate as that applied to specimens in the HVEM. After the test, the fracture surfaces were investigated by SEM and it was found that they showed the typical dimples known from bulk experiments (12). Also, polycrystalline stainless steel foils fractured in an INSTRON tensile testing machine showed the typical dimples down to a foil thickness of 3.7×10^{-4} cm which was the lowest thickness in the macroscopical foil test (10). Thus, it is concluded that the general features of void initiation and void growth are not dependent on thickness down to about 2×10^{-4}cm.

With increasing void growth the material between the voids changes its shape depending on the fracture mode in operation. A recent review by Beachem (17) has clarified the relationship between dimple shapes and fracture modes; he has shown by analyzing matching fracture surfaces with SEM that the dimple length on the two surfaces need not be the same. Amongst other things Beachem concluded that there are differences in direction and relative degree of plastic flow at the crack tip. In order to continue plastic deformation, a large mobile dislocation density must be available. Our observations by HVEM have shown that the growing holes have edges containing many slip steps as well as "rounded" corners but develop to almost perfect parallelograms at the instance of coalescence. It is a result of considerable importance that during the process of straining large numbers of dislocations are seen moving through the ligament but that at rest ligaments are free of dislocations. The reason for this becomes clear when considering the stress τ needed to operate a dislocation source:

$$\tau = \frac{Gb}{\ell}$$

where ℓ is the distance between the anchoring points of a dislocation link. Since the ligament is thinner than the surrounding material it is obvious that the sources operate in the latter and that large numbers of dislocations will leave through the surface of the microcrack. The specimen fractured in the HVEM happens to be a ribbon and the glide geometry is relatively simple (13) although the hole grows in a rather complex stress field. In bulk specimens, the voids are predominantly spherical or ellipsoidal which introduces a completely different ligament geometry that is more comparable to the stretching of hollow cylinders than flat ligaments. Since the stresses acting on voids are primarily shear stresses determined by the void sheet geometry is can thus hardly be expected that the ligaments in bulk crystal will exhibit sharp geometrical slip traces. Nevertheless, the location of sources to generate the large numbers of glide dislocations needed for the final coalescence of the voids can eventually only be in that part of the crystal that after separation has become the flank of the crack.

In conclusion it should be stated that despite the non-crystallographic appearance of fracture surfaces produced by the ductile mode, no deviations from the principles of crystal plasticity have been found in developing mechanisms for the void initiation - void growth - void coalescence sequence in the micro-structural regime. This insight should make it possible not only to aid our deeper understanding of ductile fracture but also to improve deformation processing technology.

Acknowledgement

This paper is based on the master's thesis of Robert L. Lyles, Jr. and the dissertation of Robert W. Bauer. The support of the Office of Naval Research, Metallurgy Branch, is gratefully acknowledged.

References

1. J. Gurland and J. Plateau, Trans. ASM 56, 442 (1963).

2. A. R. Rosenfield, Met. Rev. 13, 29 (1968).

3. D. Broek, Tech. Hogeschool Delft, Netherlands (1971).

4. J. D. Meakin and H. G. F. Wilsdorf, Trans. AIME 218, 737 and 745 (1960).

5. C. D. Beachem, Fracture, Ed. H. Liebowitz, Acad. Press, New York, 1968, Vol. I, 244.

6. D. Broek, Int. Met. Rev. 19, 135 (1974).

7. R. L. Patterson and H. G. F. Wilsdorf, Fracture, Ed. H. Liebowitz, Acad. Press, New York, 1968, Vol. I, 183.

8. R. W. Bauer, R. L. Lyles, Jr. and H. G. F. Wilsdorf, Zs. Metallkd. 63, 525 (1972).

9. A. S. Tetelman and A. J. McEvily, Jr., Fracture of Structural Materials, John Wiley, New York, 1967, 249.

10. R. W. Bauer and H. G. F. Wilsdorf, Proc. Int. Conf. on Dynamic Crack Propagation, Ed. G. C. Sih, Noordhoff Int. Publ., Leyden, 1973, 197.

11. R. W. Bauer and H. G. F. Wilsdorf, Scripta Met. 7, 1213 (1973).

12. R. L. Lyles, Jr., M.S. Thesis, University of Virginia, 1971.

13. R. L. Lyles, Jr. and H. G. F. Wilsdorf, Acta Met. 23, 269, 1975.

14. F. A. McClintock and A. S. Argon, Mechanical Behavior of Materials, Addison-Wesley, Reading, Mass., 1966, 524.

15. P. F. Thomason, J. Inst. Met. 96, 360 (1968).

16. H. C. Rogers, Trans. AIME 218, 498 (1960).

17. C. D. Beachem, Met. Trans. 6A, 377 (1975).

18. A. S. Tetelman, Acta Met. 12, 993 (1964).

19. B. E. Warren, Progr. Met. Phys. 8, 147 (1959).

20. R. Gasca-Neri and W. D. Nix, Acta Met. 22, 257 (1974).

21. D. Kuhlmann-Wilsdorf, R. Maddin and H. G. F. Wilsdorf, Strengthening Mechanisms in Solids, ASM, Metals Park, Ohio, 1962, 137.

22. D. Kuhlmann-Wilsdorf and H. G. F. Wilsdorf, Symposium on Electron Microscopy, Wiley and Sons, New York, 1963, 575.

23. R. W. Bauer, R. Geiss, R. L. Lyles, Jr. and H. G. F. Wilsdorf, Jerkont. Ann. 155, 407 (1971).